Article

Determination of Membrane Protein Structure and Dynamics by Magic-Angle-Spinning Solid-State NMR Spectroscopy

Ovidiu C. Andronesi, Stefan Becker, Karsten Seidel, Henrike Heise, Howard S. Young, and Marc Baldus

J. Am. Chem. Soc., **2005**, 127 (37), 12965-12974• DOI: 10.1021/ja0530164 • Publication Date (Web): 26 August 2005

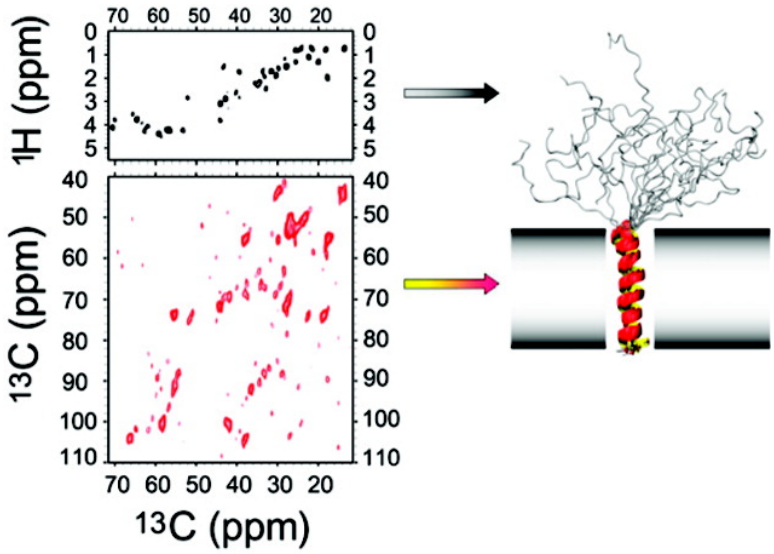

More About This Article

Additional resources and features associated with this article are available within the HTML version:

- Supporting Information
- Links to the 26 articles that cite this article, as of the time of this article download
- Access to high resolution figures
- Links to articles and content related to this article
- Copyright permission to reproduce figures and/or text from this article

View the Full Text HTML

J|A|C|S
ARTICLES
Published on Web 08/26/2005

Determination of Membrane Protein Structure and Dynamics by Magic-Angle-Spinning Solid-State NMR Spectroscopy†

Ovidiu C. Andronesi,‡ Stefan Becker,‡ Karsten Seidel,‡ Henrike Heise,‡ Howard S. Young,§ and Marc Baldus*,‡

Contribution from the Department of NMR-based Structural Biology, Max-Planck-Institute for Biophysical Chemistry, Am Fassberg 11, 37077 Göttingen, Germany, and Department of Biochemistry, University of Alberta, Edmonton, Alberta T6G 2H7, Canada

Received May 9, 2005; E-mail: maba@mpibpc.mpg.de

Abstract: It is shown that molecular structure and dynamics of a uniformly labeled membrane protein can be studied under magic-angle-spinning conditions. For this purpose, dipolar recoupling experiments are combined with novel through-bond correlation schemes that probe mobile protein segments. These NMR schemes are demonstrated on a uniformly [^{13}C,^{15}N] variant of the 52-residue polypeptide phospholamban. When reconstituted in lipid bilayers, the NMR data are consistent with an α-helical trans-membrane segment and a cytoplasmic domain that exhibits a high degree of structural disorder.

1. Introduction

For a long time, nuclear magnetic resonance (NMR) techniques have provided information on structural propensities and dynamics of partially disordered proteins in solution.[1,2] The occurrence of such unstructured regions is surprisingly common in functional proteins[3] and relevant in crucial areas such as transcriptional regulation, translation, and cellular signal transduction.[3,4] As for membranes and membrane-associated proteins, the increase in molecular size and tumbling rate can prohibit the use of solution-state NMR techniques. Instead, magic-angle-spinning (MAS[5]) NMR has been shown to extend the use of standard solution-state NMR methods to characterize molecular structure and dynamics.[6,7] For larger membrane-interacting proteins, the molecular tumbling rate is further reduced and the application of solid-state NMR methods that explicitly take into account anisotropic interactions becomes mandatory.[7,8] In this regime, dipolar, chemical shielding, and quadrupolar interactions[9] provide a direct instrument to probe molecular structure. Protein dynamics can be monitored by motional averaging of the anisotropic interactions and they modulate relaxation times.[1,10] Under MAS, the topology of membranes and membrane proteins has been studied using one-dimensional ^{2}H, ^{13}C, ^{15}N, and ^{31}P NMR experiments (see, for example, refs 7, 8, 11, 12), paramagnetic quenchers,[13] and by performing deuterium−hydrogen exchange experiments.[14] In addition, two-dimensional correlation experiments that employ dipolar (i.e., through-space) transfers[15,16] and rely on the profound influence of molecular dynamics upon NMR relaxation[16,17] have been suggested. Because dipolar interactions are largely suppressed in the presence of fast molecular motion, protein structure and dynamics are often analyzed using different sample preparation methods and solid-state NMR techniques.

In the following, we present an experimental strategy to simultaneously probe protein structure and dynamics using a

† Presented in part at the 46th ENC, Rhode Island, April 10−15, 2005.
‡ Max-Planck-Institute for Biophysical Chemistry.
§ University of Alberta.

(1) Palmer, A. G.; Williams, J.; McDermott, A. *J. Phys. Chem.* **1996**, *100*, 13293−13310.
(2) Dyson, H. J.; Wright, P. E. *Chem. Rev.* **2004**, *104*, 3607−3622.
(3) Dunker, A. K.; Brown, C. J.; Lawson, J. D.; Iakoucheva, L. M.; Obradovic, Z. *Biochemistry* **2002**, *41*, 6573−6582.
(4) Dyson, H. J.; Wright, P. E. *Nat. Rev. Mol. Cell Biol.* **2005**, *6*, 197−208.
(5) Andrew, E. R.; Bradbury, A.; Eades, R. G. *Nature* **1958**, *182*, 1659.
(6) Oldfield, E.; Bowers, J. L.; Forbes, J. *Biochemistry* **1987**, *26*, 6919−6923. Bouchard, M.; Davis, J. H.; Auger, M. *Biophys. J.* **1995**, *69*, 1933−1938. Pampel, A.; Strandberg, E.; Lindblom, G.; Volke, F. *Chem. Phys. Lett.* **1998**, *287*, 468−474. Huster, D.; Kuhn, K.; Kadereit, D.; Waldmann, H.; Arnold, K. *Angew. Chem., Int. Ed.* **2001**, *40*, 1056−1057. Soubias, O.; Reat, V.; Saurel, O.; Milon, A. *J. Magn. Reson.* **2002**, *158*, 143−148. Zhang, W. Y.; Crocker, E.; McLaughlin, S.; Smith, S. O. *J. Biol. Chem.* **2003**, *278*, 21459−21466.
(7) Davis, J. H.; Auger, M. *Prog. Nucl. Magn. Reson. Spectrosc.* **1999**, *35*, 1−84.
(8) Cross, T. A.; Opella, S. J. *Curr. Opin. Struct. Biol.* **1994**, *4*, 574−581. Griffiths, J. M.; Griffin, R. G. *Anal. Chim. Acta* **1993**, *283*, 1081−1101. Smith, S. O.; Aschheim, K.; Groesbeek, M. *Q. Rev. Biophys.* **1996**, *29*, 395−449. Opella, S. J.; Marassi, F. M. *Chem. Rev.* **2004**, *104*, 3587−3606.
(9) Mehring, M. *Principles of High-Resolution NMR in solids*, 2nd ed.; Springer: Berlin, 1983.
(10) Peng, J. W.; Wagner, G. *Methods Enzymol.* **1994**, *239*, 563−596. Huster, D. *Prog. Nucl. Magn. Reson. Spectrosc.* **2005**, *46*, 79−107.
(11) Keniry, M. A.; Gutowsky, H. S.; Oldfield, E. *Nature* **1984**, *307*, 383−386.
(12) Lewis, B. A.; Harbison, G. S.; Herzfeld, J.; Griffin, R. G. *Biochemistry* **1985**, *24*, 4671−4679. Bowers, J. L.; Oldfield, E. *Biochemistry* **1988**, *27*, 5156−5161. Tuzi, S.; Naito, A.; Saito, H. *Biochemistry* **1994**, *33*, 15046−15052. Engelhard, M.; Finkler, S.; Metz, G.; Siebert, F. *Eur. J. Biochem.* **1996**, *235*, 526−533. Creuzet, F.; McDermott, A.; Gebhard, R.; Vanderhoef, K.; Spijkerassink, M. B.; Herzfeld, J.; Lugtenburg, J.; Levitt, M. H.; Griffin, R. G. *Science* **1991**, *251*, 783−786. Mason, A. J.; Turner, G. J.; Glaubitz, C. *FEBS J.* **2005**, *272*, 2152−2164.
(13) Brown, L. R.; Braun, W.; Kumar, A.; Wuthrich, K. *Biophys. J.* **1982**, *37*, 319−328. Villalain, J. *Eur. J. Biochem.* **1996**, *241*, 586−593. Tuzi, S.; Hasegawa, J.; Kawaminami, R.; Naito, A.; Saito, H. *Biophys. J.* **2001**, *81*, 425−434.
(14) Tian, C. L.; Gao, P. F.; Pinto, L. H.; Lamb, R. A.; Cross, T. A. *Protein Sci.* **2003**, *12*, 2597−2605.
(15) Gross, J. D.; Warschawski, D. E.; Griffin, R. G. *J. Am. Chem. Soc.* **1997**, *119*, 796−802. Huster, D.; Yao, X. L.; Hong, M. *J. Am. Chem. Soc.* **2002**, *124*, 874−883.
(16) Kumashiro, K. K.; Schmidt-Rohr, K.; Murphy, O. J.; Ouellette, K. L.; Cramer, W. A.; Thompson, L. K. *J. Am. Chem. Soc.* **1998**, *120*, 5043−5051.
(17) Torchia, D. A. *Annu. Rev. Biophys. Bioeng.* **1984**, *13*, 125−144.

single, uniformly (^{13}C,^{15}N) labeled membrane protein sample under MAS conditions. For this purpose, we combine dipolar transfer schemes well established under MAS conditions[18,19] with solid-state NMR experiments that invoke through-bond transfer to probe protein dynamics on a fast time scale. In principle, through-bond polarization transfer can also be established for solid-phase samples.[20−22] To distinguish different motional regimes, we select a heteronuclear through-bond polarization transfer step that is sensitive to proton T_2 relaxation and hence to variations in molecular dynamics.[23]

Our experiments are demonstrated on the monomeric form of the 52-residue protein phospholamban (AFA-PLN) that plays an important role in cardiac contractility[24] and modulates the active transport of calcium into the lumen of the sarcoplasmic reticulum by the Ca-ATPase (SERCA). SERCA enzymes belong to the class of P-type ATPases and undergo a reversible cycle of ATP hydrolysis and Ca^{2+} transport. PLN interacts with and, at low Ca^{2+} concentrations, reversibly inhibits the activity of SERCA2a (see, for example, ref 25). While PLN can self-associate to a pentameric structure in membranes,[26−28] the monomeric form is primarily responsible for the inhibition of SERCA2a[27,29] and can be stabilized in a fully functional mutant containing A36, F41, and A46 instead of three cysteine residues (AFA-PLN). Structural models of monomeric AFA-PLN were first obtained from NMR studies in organic solvents[30,31] and, more recently, in detergent micelles.[32] According to these reports, AFA-PLN comprises two α-helical domains connected by a semi-flexible hinge region. On the other hand, mutagenesis studies[33] and biophysical measurements[28,34] imply that PLN dynamics play an important role in the functional interaction of PLN and Ca-ATPase. Spectroscopic evidence that the cytoplasmic domain of PLN may indeed adopt, at least transiently, an unstructured conformation[25] comes from FTIR experiments on wild-type PLN[35] and from EPR experiments on spin-labeled AFA-PLN mutants in lipid bilayers.[36] According to the latter experiments, the cytoplasmic domain of AFA-PLN exists in a dynamic equilibrium of two conformational states described by a moderately stable α-helix and a significantly populated unstructured ensemble.

As compared to solid-state NMR investigations performed on specifically labeled samples of truncated,[37] full length wild-type,[38] or monomeric mutant[39,40] PLN, two-dimensional solid-state NMR experiments shown in the following offer the advantage of simultaneously probing molecular structure and dynamics along the complete polypeptide sequence. Our experiments suggest that a significant population of monomeric phospholamban exists in liposomes that is characterized by an α-helical trans-membrane segment and a cytoplasmic domain that exhibits a high degree of structural disorder.

2. Experimental Methods

Materials. Deuterated dimyristoylphosphatidylcholine (DMPC-D67), dioleoylphosphatidylcholine (DOPC), and dioleoylphosphatidylethanolamine (DOPE) were purchased from Avanti Polar Lipids (Alabaster, AL) and used without further purification. Uniformly (^{13}C,^{15}N) labeled recombinant AFA-PLN was obtained according to ref 41. Briefly, AFA-PLN was expressed in *E. coli* as a C-terminal fusion to maltose binding protein (MBP) with a pre-engineered TEV protease cleavage site between MBP and AFA-PLN. Protein expression was performed in minimal labeling medium containing [^{15}N]-NH_4Cl and [$^{13}C_6$]-D-glucose as the only nitrogen and carbon sources. After cell lysis by sonication, the MBP-fusion protein was purified by amylose-affinity chromatography and subsequently digested with TEV protease. The released AFA-PLN protein formed a precipitate that was taken up in 7 M guanidine-hydrochloride and further purified to homogeneity by reverse-phase HPLC using a 0.05% TFA−2-propanol solvent system. Due to the TEV cleavage site and the cloning strategy, the recombinant AFA-PLN protein contains an additional N-terminal GS motif. The amino acid sequence (G_1S MEKVQYLTRS AIRRASTIEM PQQARQKLQN LFINFALILI FLLLIAIIVM LL_{54}) differs from Pollesello et al.[30] by the absence of cysteine residues and the length. Except for the N-terminal GS motif, our amino acid sequence represents human PLN and largely resembles the polypeptide used in ref 32 (PDB code: 1N7L). It differs from ref 31 (PDB entries: 1FJK, 1FJP) by, in total, 6 residues, including two cysteines.

Sample Preparation. DMPC[38,39] and a 4:1 mixture of DOPC/DOPE[36] can be used for functional reconstitution of phospholamban into lipid bilayers as determined by ATPase activity.[42] Proteoliposomes containing U-[^{13}C,^{15}N] labeled AFA-PLN were prepared as follows: $CHCl_3$/MeOH 1:1 (100 μL) was used to dissolve 3.4 mg of U-[^{13}C,^{15}N]-labeled AFA-PLN in 8 mg of DMPC-D67 ($CHCl_3$/MeOH 1:1, 50 μL) to give a lipid to protein molar ratio (L/P) of 20:1. The mixture was vortexed, dried under a stream of N_2, and stored under high vacuum overnight to remove all residual solvent. Subsequently, the sample was hydrated with 30 μL of NaPi buffer pH 7.0 and transferred to a 4 mm MAS rotor, frozen at −80 °C, and lyophilized. Next, 10 μL of H_2O was used for rehydration. An additional sample was prepared using 1 mg of U-[^{13}C,^{15}N] labeled AFA-PLN in 50 μL of $CHCl_3$/MeOH 1:1 and 12.2 mg of DMPC-D67 to give a L/P ratio of 100:1. Finally, 7 mg

(18) Griffin, R. G. *Nat. Struct. Biol.* **1998**, *5*, 508−512.
(19) Egorova-Zachernyuk, T. A.; Hollander, J.; Fraser, N.; Gast, P.; Hoff, A. J.; Cogdell, R.; de Groot, H. J. M.; Baldus, M. *J. Biomol. NMR* **2001**, *19*, 243−253.
(20) Baldus, M.; Meier, B. H. *J. Magn. Reson., Ser. A* **1996**, *121*, 65−69. Baldus, M.; Iuliucci, R. J.; Meier, B. H. *J. Am. Chem. Soc.* **1997**, *119*, 1121−1124.
(21) Lesage, A.; Auger, C.; Caldarelli, S.; Emsley, L. *J. Am. Chem. Soc.* **1997**, *119*, 7867−7868.
(22) Lesage, A.; Charmont, P.; Steuernagel, S.; Emsley, L. *J. Am. Chem. Soc.* **2000**, *122*, 9739−9744.
(23) Schmidt-Rohr, K.; Spiess, H. W. *Multidimensional Solid-state NMR and Polymers*; Academic Press: London/San Diego, 1994.
(24) MacLennan, D. H.; Kranias, E. G. *Nat. Rev. Mol. Cell Biol.* **2003**, *4*, 566−577.
(25) MacLennan, D. H.; Abu-Abed, M.; Kang, C. *J. Mol. Cell. Cardiol.* **2002**, *34*, 897−918.
(26) Adams, P. D.; Arkin, I. T.; Engelman, D. M.; Brunger, A. T. *Nat. Struct. Biol.* **1995**, *2*, 154−162. Ying, W. W.; Irvine, S. E.; Beekman, R. A.; Siminovitch, D. J.; Smith, S. O. *J. Am. Chem. Soc.* **2000**, *122*, 11125−11128.
(27) Reddy, L. G.; Jones, L. R.; Thomas, D. D. *Biochemistry* **1999**, *38*, 3954−3962.
(28) Cornea, R. L.; Jones, L. R.; Autry, J. M.; Thomas, D. D. *Biochemistry* **1997**, *36*, 2960−2967.
(29) Kimura, Y.; Kurzydlowski, K.; Tada, M.; MacLennan, D. H. *J. Biol. Chem.* **1997**, *272*, 15061−15064.
(30) Pollesello, P.; Annila, A.; Ovaska, M. *Biophys. J.* **1999**, *76*, 1784−1795.
(31) Lamberth, S.; Schmid, H.; Muenchbach, M.; Vorherr, T.; Krebs, J.; Carafoli, E.; Griesinger, C. *Helv. Chim. Acta* **2000**, *83*, 2141−2152.
(32) Zamoon, J.; Mascioni, A.; Thomas, D. D.; Veglia, G. *Biophys. J.* **2003**, *85*, 2589−2598.
(33) Toyofuku, T.; Kurzydlowski, K.; Tada, M.; Maclennan, D. H. *J. Biol. Chem.* **1994**, *269*, 3088−3094.
(34) Kirby, T. L.; Karim, C. B.; Thomas, D. D. *Biochemistry* **2004**, *43*, 5842−5852.
(35) Tatulian, S. A.; Jones, L. R.; Reddy, L. G.; Stokes, D. L.; Tamm, L. K. *Biochemistry* **1995**, *34*, 4448−4456.
(36) Karim, C. B.; Kirby, T. L.; Zhang, Z. W.; Nesmelov, Y.; Thomas, D. D. *Proc. Natl. Acad. Sci. U.S.A.* **2004**, *101*, 14437−14442.
(37) Dave, P. C.; Tiburu, E. K.; Damodaran, K.; Lorigan, G. A. *Biophys. J.* **2004**, *86*, 1564−1573.
(38) Smith, S. O.; Kawakami, T.; Liu, W.; Ziliox, M.; Aimoto, S. *J. Mol. Biol.* **2001**, *313*, 1139−1148.
(39) Hughes, E.; Middleton, D. A. *J. Biol. Chem.* **2003**, *278*, 20835−20842.
(40) Mascioni, A.; Karim, C.; Zamoon, J.; Thomas, D. D.; Veglia, G. *J. Am. Chem. Soc.* **2002**, *124*, 9392−9393.
(41) Douglas, J. L.; Trieber, C. A.; Afara, M.; Young, H. S. *Protein Expression Purif.* **2005**, *40*, 118−125.
(42) Dalton, K. A.; Pilot, J. D.; Mall, S.; East, J. M.; Lee, A. G. *Biochem. J.* **1999**, *342*, 431−438.

of U-[^{13}C,^{15}N]-labeled AFA-PLN was dissolved in 300 μL of $CHCl_3$/MeOH (1:1) and combined with 16.5 mg of DOPC/DOPE (molar ratio 4:1) in 500 μL of $CHCl_3$ (L/P = 20:1) and vortexed. After being dried under a stream of N_2, the mixture was stored under high vacuum overnight to remove residual solvent. The sample was hydrated with 30 μL of H_2O and transferred to a 4 mm MAS rotor. To investigate any potential influence of lyophilization that was previously used during protein reconstitution of phospholamban[43] and of other membrane peptides,[44] we recorded INEPT data on AFA-PLN in DOPC/DOPE liposomes before and after lyophilization and rehydration. No changes in the spectra were observed. ^{31}P NMR experiments confirm that all spectra were recorded in the liquid crystalline phase using MAS rates between 5 and 11 kHz. Within this range of spinning speeds, no variations of the ^{1}H and (proton-decoupled) ^{13}C one-quantum line width were observed. Additional test experiments furthermore indicate that the structural data obtained are independent of the lipid-to-protein ratio in the range L/P = 20:1 to L/P = 100:1 for the two lipid compositions considered (see Supporting Information). For simplicity, only data using DMPC-D67 liposomes are shown in the following.

NMR Experiments. All solid-state NMR experiments were conducted on NMR instruments (Bruker Biospin, Germany) using a 4 mm triple resonance (^{1}H,^{13}C,^{15}N) MAS probehead at 18.8 T (^{1}H resonance frequency 800 MHz, standard bore), 14.1 T (600 MHz, wide bore), and 9.4 T (400 MHz, wide bore) at a temperature of 30 °C (DMPC) and 5 °C (DOPC/DOPE). Through-space transfer experiments involved broad-band (^{1}H,^{13}C) and chemical-shift selective[45] (^{15}N→^{13}C) Hartmann−Hahn[46] cross polarization schemes. SPINAL64[47] and GARP[48] proton decoupling was applied during through-space and through-bond (vide infra) correlation experiments using radio frequency (rf) fields of 75 and 10 kHz, respectively. For dipolar double-quantum excitation, the SPC5[49] scheme was used. Sequential (^{15}N,^{13}C) resonance assignments were obtained using NCACB and NCOCA type correlation experiments described earlier.[19,50,51]

NMR Schemes To Detect Mobile Protein Segments under MAS. Complementary to dipolar mixing units, we present in Figure 1 a series of two- and three-dimensional experiments to probe mobile protein segments under MAS conditions. For brevity, the pulse schemes depicted in Figure 1 will be denoted in the following by (a) HCC, (b) HHC or HHN, (c) HNCACB or HNCOCACB, and (d) HNHHC. In all cases, polarization transfer schemes are used that facilitate through-bond polarization transfer without reintroduction of (through-space) dipolar interactions. As reviewed elsewhere,[18] such through-space interactions can be reintroduced using a variety of rotor-synchronized rf schemes. While for homonuclear polarization transfer, these requirements have led to the development of TOBSY polarization transfer schemes,[20,52] we employ for all heteronuclear transfer steps a refocused INEPT[53] experiment. Using average Hamiltonian theory,[54] it can easily be shown that dipolar interactions vanish under this mixing unit and only through-bond polarization transfer is active. This scheme selects proton signals with long T_2 relaxation times and hence probes mobile protein segments.[23]

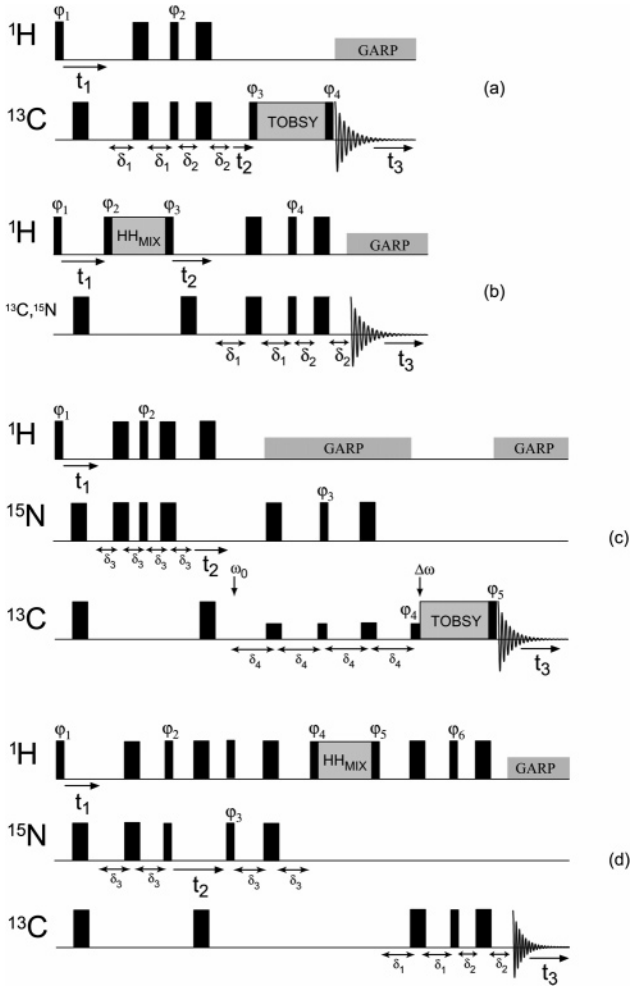

Figure 1. Double- and triple-channel pulse sequences for two- or three-dimensional NMR experiments to detect mobile protein segments under MAS conditions: (a) HCC, (b) HHC or HHN, (c) HNCACB or HNCOCACB, and (d) HNHHC. Unless stated otherwise, narrow and wide black rectangles correspond to 90° and 180° pulses, respectively. Heteronuclei (^{13}C or ^{15}N) are detected under ^{1}H decoupling (GARP[48]). In (a), intraresidue through-bond HCC correlations are obtained via longitudinal isotropic broad-band (^{13}C,^{13}C) mixing with TOBSY[20] using the P9$^1_3$ sequence.[52] In (b), proton−proton mixing (such as NOESY[55] or TOBSY mixing) is used to detect HHC or HHN correlations. Sequential assignments are obtained via HNCACB and HNCOCACB experiments shown in (c). Finally, through-space correlations can be probed in the HNHHC experiment of (d) with HH$_{MIX}$ = NOESY. Pulses with indicated phases φ_i are cycled in steps of 180° except for φ_4 in (a) and φ_5 in (c) that are incremented by 90°.

In Figure 1a, intraresidue through-bond HCC correlations are recorded. Polarization is first transferred from ^{1}H to a directly bonded ^{13}C nucleus and subsequently relayed via a (^{13}C,^{13}C) scalar coupling to the chemically bonded ^{13}C. For TOBSY mixing, we employed the P9$^1_3$ sequence.[52] In (b), proton−proton polarization transfer is recorded using rare-spin detection (i.e., ^{13}C or ^{15}N). Mixing can relate to through-space (e.g., NOESY[55]) or through-bond (HH$_{MIX}$ = TOBSY) transfer units. Sequential assignments are obtained via HNCACB and HNCOCACB experiments depicted in (c). For selective NCO or NCA INEPT transfer, weak, on-resonance ^{13}C pulses are used. For HNCOCACB-type correlations, the ^{13}C carrier frequency (ω_0) is put on resonance for CO during NCO transfer and set in the middle of the CO−CA region ($\Delta\omega$) during TOBSY mixing and detection. For NCA transfer, the ^{13}C carrier is placed on resonance for CA nuclei. Finally, through-space correlations can be probed also in the HNHHC experiment

(43) Ying, W. W.; Irvine, S. E.; Beekman, R. A.; Siminovitch, D. J.; Smith, S. O. *J. Am. Chem. Soc.* **2000**, *122*, 11125−11128.
(44) Fu, R. Q.; Cotten, M.; Cross, T. A. *J. Biomol. NMR* **2000**, *16*, 261−268.
(45) Baldus, M.; Petkova, A. T.; Herzfeld, J.; Griffin, R. G. *Mol. Phys.* **1998**, *95*, 1197−1207.
(46) Hartmann, S. R.; Hahn, E. L. *Phys. Rev.* **1962**, *128*, 2042−2053.
(47) Fung, B. M.; Khitrin, A. K.; Ermolaev, K. *J. Magn. Reson.* **2000**, *142*, 97−101.
(48) Shaka, A. J.; Barker, P. B.; Freeman, R. *J. Magn. Reson.* **1985**, *64*, 547−552.
(49) Hohwy, M.; Rienstra, C. M.; Jaroniec, C. P.; Griffin, R. G. *J. Chem. Phys.* **1999**, *110*, 7983−7992.
(50) Pauli, J.; Baldus, M.; van Rossum, B.; de Groot, H.; Oschkinat, H. *ChemBioChem* **2001**, *2*, 272−281.
(51) Baldus, M. *Prog. Nucl. Magn. Reson. Spectrosc.* **2002**, *41*, 1−47.
(52) Hardy, E. H.; Verel, R.; Meier, B. H. *J. Magn. Reson.* **2001**, *148*, 459−464.
(53) Morris, G. A.; Freeman, R. *J. Am. Chem. Soc.* **1979**, *101*, 760−762.
(54) Haeberlen, U. In *Advances in Magnetic Resonance*; Waugh, J. S., Ed.; Academic Press: New York, 1976.
(55) Jeener, J.; Meier, B. H.; Bachmann, P.; Ernst, R. R. *J. Chem. Phys.* **1979**, *71*, 4546−4553.

depicted in (d) with HH_{MIX} = NOESY when spectral overlap is severe in the corresponding HHN or HHC variants shown in Figure 1b. As compared to schemes designed for liquid-state applications in two[56] or three[57] spectral dimensions, all sequences hence use rf mixing units that minimize the influence of unwanted dipolar interactions and involve the detection of ^{13}C or ^{15}N resonances.[56] For the applications discussed in the following, direct proton detection in the acquisition dimension was prohibited by the occurrence of strong water signals. MAS probeheads using pulsed field gradients are likely to alleviate these shortcomings.

Structural Analysis. Structure calculations were performed using a simulated annealing protocol in CNS[58] version 1.1 with the PROTEIN-ALLHDG parameter file.[59] In line with earlier studies[30−32] and results of the HHC experiment (vide infra), structures containing the N-terminal domain (residues 1−23) that penetrates the lipid bilayer were excluded during the calculations. Cα and Cβ chemical shift assignments were used to establish backbone dihedral angle constraints in TALOS,[60] and proton−proton distance constraints were derived from an HHC spectrum. As described earlier,[61,62] square-well potentials were employed to represent experimental constraints in the simulation. No constraint force was applied for proton−proton distances below 5 Å, and backbone torsion angle deviations from the TALOS prediction within a range given by the prediction RMSD for both angles ("flat bottoms"). As starting conformation for all simulations, an extended strand of AFA-PLN was generated from the amino acid sequence. The structure calculation protocol consisted of three stages: (1) High-temperature annealing in torsion angle space, in 2000 time steps of 0.015 ps at 50 000 K; (2) slow-cool annealing in torsion angle space, in 4000 steps of 0.015 ps, and temperature reduction from 50 000 K to zero in steps of 250 K; and (3) final conjugate gradient minimization in 10 cycles of 200 steps each. Distance constraints were invoked by force constants of 300 kcal mol^{-1} $Å^{-2}$ during annealing and halved for conjugate gradient minimization. Ambiguities in the assignments of methylene and methyl protons were accounted for by sum averaging over all possible contacts. From the TALOS analysis, a total of 28 (ϕ,ψ) backbone angle constraints were included. A set of 200 structures was calculated starting with different initial velocities. An ensemble of 15 structures with the lowest energy, which are in agreement with the membrane geometry, was selected to represent the molecular conformation of the PLN monomer. The structures were aligned along backbone atoms of residues L30−L53. In this ensemble, no distance or angle restraint violation of more than 0.2 Å or 2° occurred.

3. Results and Discussion

Through-Space versus Relaxation-Filtered Through-Bond Transfer. In the following, we relate experimental results obtained using schemes depicted in Figure 1 to data obtained by means of dipolar recoupling techniques on proteoliposomes containing a uniformly (^{13}C,^{15}N) labeled sample of phospholamban. In Figure 2, results of a one-dimensional through-bond (^{1}H,^{13}C) transfer experiment (refocused INEPT, red) are compared to data obtained under dipolar cross polarization (CP) (black) conditions. In both spectra, aliphatic side-chain carbon

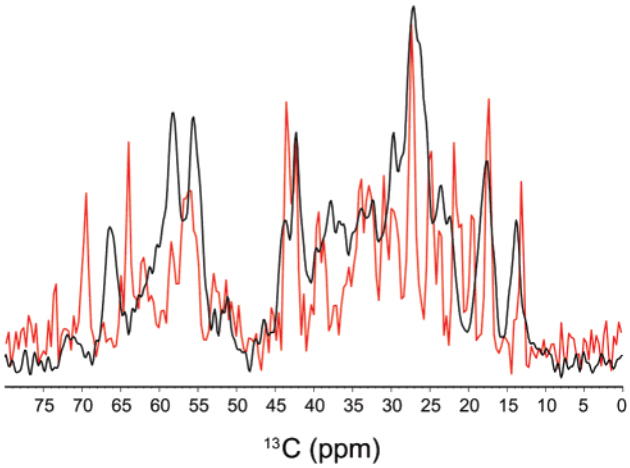

Figure 2. Comparison of a ^{13}C detected CP (black) versus INEPT (red) experiment on AFA-PLN in DMPC bilayers. Experiments were performed at 11 kHz MAS, 30 °C, and 600 MHz. A CP time of 1 ms and an INEPT transfer time optimized for a one-bond coupling of $^{1}J_{CH}$ = 155 Hz were used.

resonances are readily observed. Differences in both spectra speak in favor of variable T_2 relaxation, which is determined predominantly by dipolar proton−proton interactions. Because changes in these interactions are associated with variations in molecular dynamics,[23] we conclude from Figure 2 that phospholamban contains amino acid segments that exhibit different degrees of molecular mobility.

Large variations in signal intensity in the Cα region of Figure 2 also suggest that CP and INEPT spectra reflect polypeptide segments with different secondary structures. In addition, lipid signals can contribute differently to CP and INEPT spectra. To further investigate these aspects in detail, two-dimensional correlation experiments were conducted. In Figure 3a, we present experimental data of a two-dimensional INEPT-type experiment containing (^{1}H,^{13}C) one-bond correlations. As compared to MAS solid-state NMR experiments on rigid solids, ^{1}H line widths are largely reduced and range between 0.15 and 0.35 ppm, indicative of molecular mobility that leads to significant reduction of dipolar interactions and a concomitant decrease in proton T_2 relaxation. In Figure 3b, results of a conventional 2D (^{13}C,^{13}C) (2Q,1Q) correlation experiment using a dipolar recoupling sequence for 2Q excitation are shown for comparison. In both 2D spectra, the ^{13}C single quantum line width is comparable. As demonstrated earlier,[63] information about amino acid specific chemical shift ranges can be used to monitor individual protein residue types in the absence of sequential resonance assignments. In the case of PLN, such conditions exist for S, T, and Y residues that resonate in well-defined spectral regions of a through-bond or through-space correlation experiment displayed in Figure 3a and b, respectively. Indeed, such residue types are clearly visible in the aliphatic and aromatic region of the (through-bond) HC spectrum (Figure 3a, aromatic part of spectrum not shown). On the other hand, these residue types are missing in Figure 3b, where dipolar (^{13}C,^{13}C) polarization transfer is used. The latter observation could be explained by the occurrence of static or dynamic disorder of the considered residue types. Because Figure 3a

(56) Westler, W. M.; Stockman, B. J.; Markley, J. L. *J. Am. Chem. Soc.* **1988**, *110*, 6256−6258. Stockman, B. J.; Reily, M. D.; Westler, W. M.; Ulrich, E. L.; Markley, J. L. *Biochemistry* **1989**, *28*, 230−236.
(57) Ikura, M.; Kay, L. E.; Bax, A. *Biochemistry* **1990**, *29*, 4659−4667. Bax, A.; Grzesiek, S. *Acc. Chem. Res.* **1993**, *26*, 131−138.
(58) Brunger, A. T.; Adams, P. D.; Clore, G. M.; DeLano, W. L.; Gros, P.; Grosse-Kunstleve, R. W.; Jiang, J. S.; Kuszewski, J.; Nilges, M.; Pannu, N. S.; Read, R. J.; Rice, L. M.; Simonson, T.; Warren, G. L. *Acta Crystallogr., Sect. D* **1998**, *54*, 905−921.
(59) Nilges, M. *Curr. Opin. Struct. Biol.* **1996**, *6*, 617−623.
(60) Cornilescu, G.; Delaglio, F.; Bax, A. *J. Biomol. NMR* **1999**, *13*, 289−302.
(61) Lange, A.; Seidel, K.; Verdier, L.; Luca, S.; Baldus, M. *J. Am. Chem. Soc.* **2003**, *125*, 12640−12648.
(62) Lange, A.; Becker, S.; Seidel, K.; Giller, K.; Pongs, O.; Baldus, M. *Angew. Chem., Int. Ed.* **2005**, *44*, 2089−2092.
(63) Luca, S.; White, J. F.; Sohal, A. K.; Filippov, D. V.; van Boom, J. H.; Grisshammer, R.; Baldus, M. *Proc. Natl. Acad. Sci. U.S.A.* **2003**, *100*, 10706−10711.

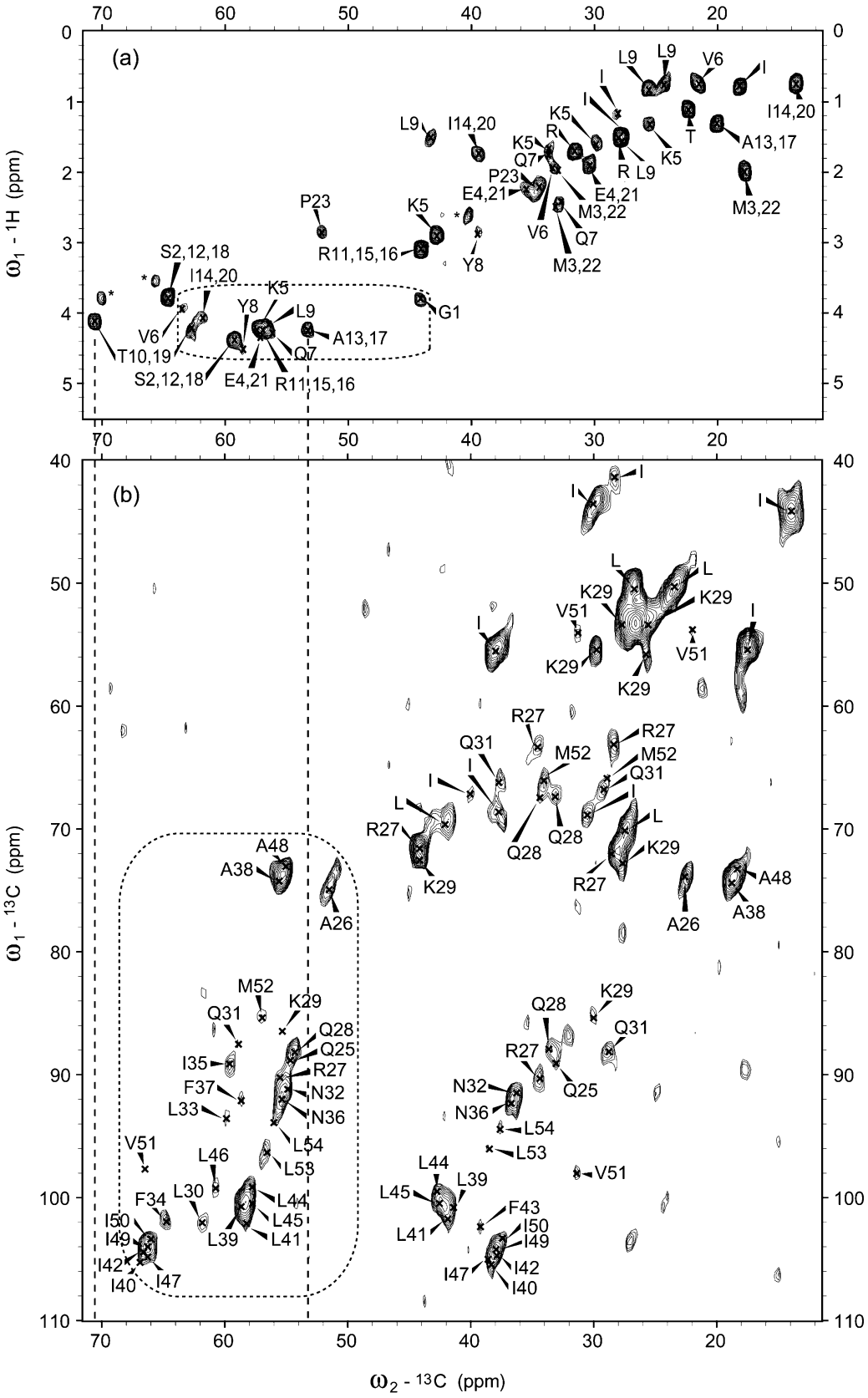

Figure 3. Results of an HC-INEPT experiment (a) and a double quantum CC experiment (b) on a uniformly labeled sample of AFA-PLN (L/P = 20:1). Experiments were conducted at 600 MHz using MAS rates of 9 and 7.5 kHz for (a) and (b), respectively. Experimental conditions in (a) were optimized for a $^1J_{CH}$ coupling constant of 155 Hz. 640 scans for each t_1 experiment (total ^{1}H t_1 evolution time 4.2 ms) were acquired. In (b), a CP time of 250 μs and SPC5 DQ excitation and reconversion time of 534 μs were used. 1360 scans were averaged for each of the 55 t_1 experiments. The t_1 time increment was set to 1/4 of a rotor period (124 ppm spectral width). Both data sets were Fourier transformed using 1k zero filling in both dimensions with QSINE = 3.5 apodization window and linear prediction to one-half of the experimental points acquired in t_1. Indicated resonance assignments were obtained from NMR data sets shown below. Contributions from natural abundance lipid background are marked "*" in (a). Cα regions of the two spectra are highlighted by dashed boxes.

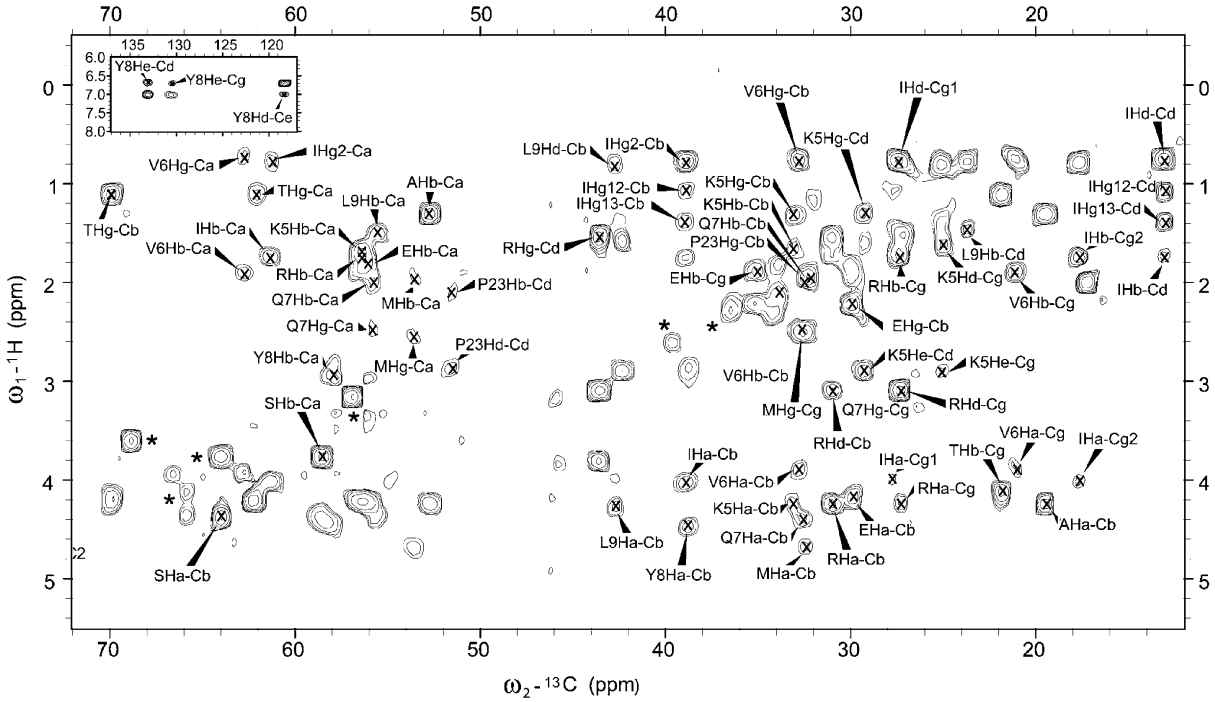

Figure 4. Results of a HCC 2D experiment (conducted at 600 MHz) using the pulse sequence given in Figure 1a. An MAS rate of 8.33 kHz and a TOBSY mixing time of 6 ms were employed. The spectrum was recorded at 30 °C using 320 scans per t_1 increment. Data were processed as in Figure 3. For the sake of clarity, only intraresidue (^{13}C,^{13}C) correlations resulting from the TOBSY transfer step are indicated. Correlations involving aromatic resonances of Y8 are shown as an inset.

contains the corresponding NMR signals, these residue types must be located in protein regions that exhibit a high degree of molecular mobility that does not affect through-bond transfer but reduces the influence of dipolar interactions. As exemplified in Figure 3 by vertical lines, such differences are not only observed for Thr residues but are also found for correlations involving Alanine.

To further characterize the resonances observed in Figure 3a and to obtain intraresidue assignments, we utilized the HCC pulse scheme shown in Figure 1a. As noted earlier, polarization is first transferred from ^{1}H to a directly bonded ^{13}C nucleus and subsequently relayed via a (^{13}C,^{13}C) scalar coupling to the chemically bonded ^{13}C. Due to faster T_2 relaxation, (^{13}C,^{13}C) homonuclear through-bond mixing schemes that contain, as in the case of INADEQUATE,[64] free precession periods were not successful. Recorded in two dimensions, the solid-state NMR spectrum hence contains intraresidue HCC correlations (t_2 evolution omitted, Figure 4). When recorded in 3D, chemical shift patterns diagnostic for each residue type can be identified. Analysis of the corresponding NMR data sets (see Supporting Information) reveals that all residue types, which according to earlier studies[30−32] should be located in the cytoplasmic domain of PLN, can be identified in a through-bond HCC experiment. These results again underline that the cytoplasmic domain exhibits a significant degree of molecular mobility. Relative to the N-terminus, the last residue still visible in the INEPT experiment but absent in the dipolar driven correlation experiment is P23.

Sequential Resonance Assignments. To obtain unequivocal sequential resonance assignments for AFA-PLN in liposomes, we combined through-space and through-bond (^{15}N,^{13}C) correlations methods as follows: First, we employed through-bond HNCOCACB and HNCACB (Figure 1c, t_1 evolution dimension omitted) experiments leading to spectra shown in Figure 5a and b, respectively. These spectra contain protein resonances that have already been identified in Figure 3a as mobile protein segments. The combination of Figures 4, 5a, and 5b leads to resonance assignments of residues 1−23 of AFA-PLN. Because no correlations consistent with the C-terminal part of AFA-PLN appear, mobile segments seen in Figures 2−5 are not due to protein segments incorrectly reconstituted into the lipid bilayer. Notably, the experimentally detected sensitivity for scalar NCO transfer is about 2-fold higher than that for NCA transfer, in line with solution-state experiments.[65] In a manner similar to Figure 5, signal sets resulting from dipolar polarization transfer were recorded using dipolar NCA and NCOCA type correlation experiments described earlier.[51] The corresponding data are shown in Figure 6a and b. Here, experiments involved dipolar SPECIFIC CP[45] and CC dipolar double-quantum polarization transfer steps. As is visible from Figure 6, the experimental spectra exhibit ^{15}N and ^{13}C line widths of 1.5 and 1 ppm, respectively. These values compare favorably to results obtained earlier in microcrystalline globular proteins[50,66] and a membrane protein complex.[19] Combined with (^{13}C,^{13}C) double quantum spectrum shown in Figure 3b, sequential resonance assignments can be obtained. Complementary to the experimental results obtained from through-bond experiments, the resulting (^{15}N,^{13}C) assignments (see Table 1, Supporting Information) only relate to the trans-membrane domain of PLN.

(64) Bax, A.; Freeman, R.; Kempsell, S. P. *J. Am. Chem. Soc.* **1980**, *102*, 4849−4851.
(65) Sattler, M.; Schleucher, J.; Griesinger, C. *Prog. Nucl. Magn. Reson. Spectrosc.* **1999**, *34*, 93−158.
(66) Böckmann, A.; Lange, A.; Galinier, A.; Luca, S.; Giraud, N.; Heise, H.; Juy, M.; Montserret, R.; Penin, F.; Baldus, M. *J. Biomol. NMR* **2003**, *27*, 323−339.

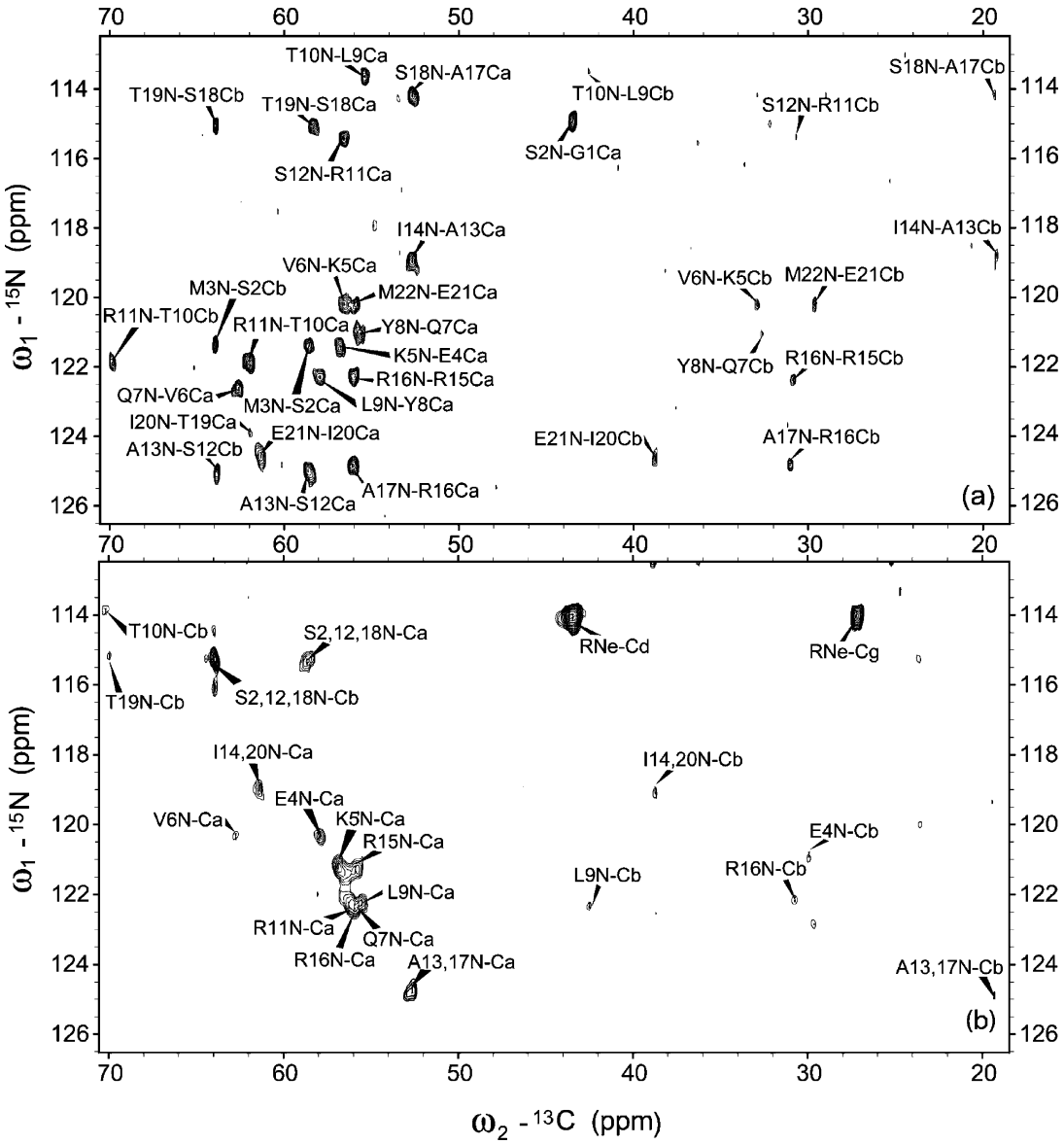

Figure 5. Sequential assignment of the cytoplasmic domain using 2D (H)NCOCACB (a) and (H)NCACB (b) spectra. Experiments were performed at 30 °C (800 MHz) using an MAS rate of 8.33 kHz. Scalar couplings of 93 Hz (HN) and 19 Hz (NC) were used for the INEPT steps. For NC selective INEPT transfer, weak (10 kHz) rectangular ^{13}C pulses were used. TOBSY ($P9^1_3$) mixing times of 8.5 ms (COCA) and 6 ms (CACB) were employed, using a 50 kHz ^{13}C rf field. 512 scans for 51 t_1 experiments (NCOCACB, 20 ppm ^{15}N spectral width) and 864 scans for 36 t_1 experiments (NCACB, 15 ppm ^{15}N spectral width) were recorded. The acquisition time was set to 20 ms using GARP ^{1}H decoupling at 10 kHz. Both spectra were processed with a QSINE = 3 apodization function.

These results suggest that the polypeptide chain of PLN exhibits domains of different molecular mobility when reconstituted into DMPC bilayers. For further characterization of the mobile protein segments, we employed the HHC pulse scheme shown in Figure 1b. As compared to Figure 1a, additional correlations that result from proton−proton interactions, which may include lipid molecules, can now be probed. In Figure 7, experimental results are shown for a longitudinal proton−proton mixing time of 300 ms. A significant number of additional correlations can be observed, albeit with lower signal intensity due to T_1 relaxation during mixing. These include inter-residue correlations such as K5−E4, T10−R11, M22−P23, and M22−I20. Notably, a large number of correlations are observed at the proton resonance frequency of H_2O (4.7 ppm), indicative of polarization exchange between peptide backbone and side-chain resonances with H_2O protons. Such correlations could indicate that the vast majority of protein residues identified in Figures 3a, 4, and 6 are exposed to an aqueous environment. Hence, side-chain hydration occurs in most N-terminal PLN residues irrespective of their hydrophobicity. Previously, such behavior was observed for soluble proteins and has been attributed to random coil character of the corresponding protein segment.[67] In principle, proton−proton interactions for protein regions that are described by sizable dipolar couplings could be further characterized using indirect detection schemes.[61,68]

Additional test experiments reveal that changes in MAS rate (above 5 kHz) have little effect upon the efficiency of INEPT-based correlation experiments and the observed ^{1}H line width. On the other hand, two-dimensional (^{1}H,^{13}C) correlation experiments using CP transfer and proton−proton (i.e., Lee−Goldburg[69]) decoupling reveal trans-membrane correlations with

(67) Otting, G.; Liepinsh, E.; Wuthrich, K. *Science* **1991**, *254*, 974−980.
(68) Lange, A.; Luca, S.; Baldus, M. *J. Am. Chem. Soc.* **2002**, *124*, 9704−9705.

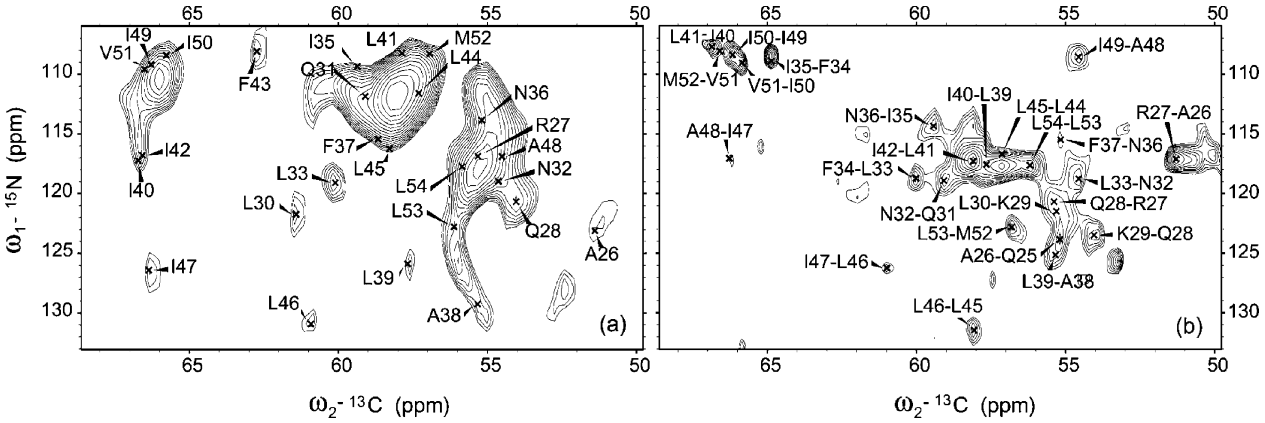

Figure 6. (a) Results of an NCA correlation experiment on U-[^{13}C,^{15}N] AFA-PLN using SPECIFIC CP[45] at 600 MHz and 7.5 kHz MAS. 4k scans were averaged for each of the 16 t_1 experiments (40 ppm spectral width). Rf fields during NCA SPECIFIC CP were 25 kHz on ^{15}N and 17.5 kHz on ^{13}C for a CP time of 5 ms. Additional experimental settings as in Figure 3 were used. (b) The 2D NCOCA was recorded under the same experimental conditions except for a 3 ms NCO SPECIFIC CP time. For dipolar (CO,CA) transfer, an SPC5 mixing time of 1.06 ms was employed. 11k scans were averaged for each of the 11 t_1 experiments (35 ppm spectral width) yielding a similar total ^{15}N evolution time in both experiments.

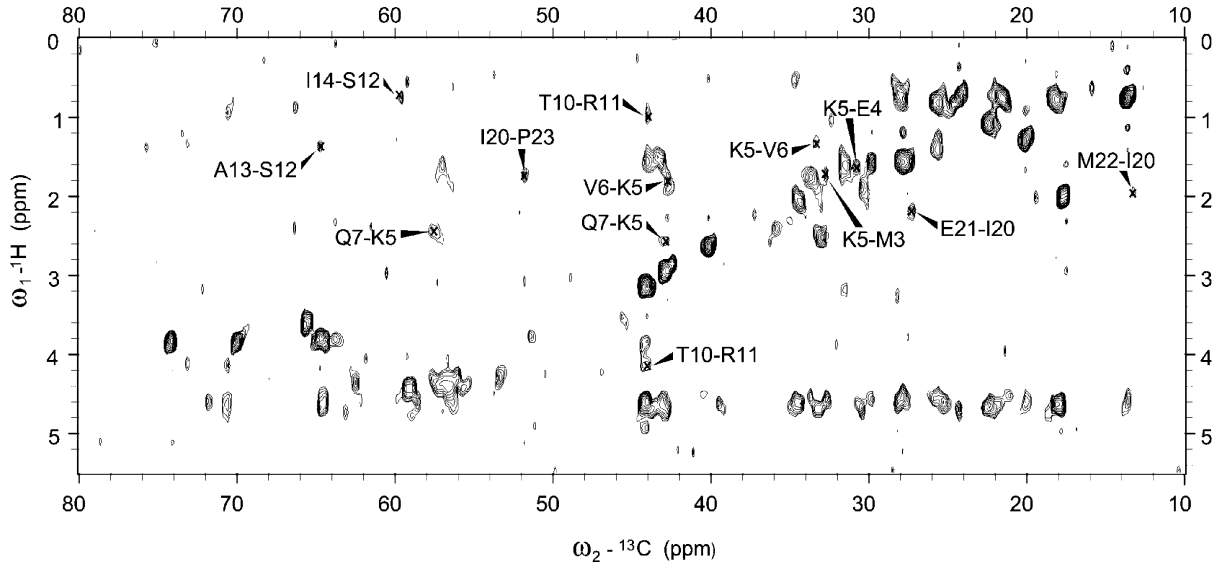

Figure 7. Results of a 2D HHC correlation experiment using the pulse sequence from Figure 1b on U-[^{13}C,^{15}N] AFA-PLN. A proton−proton mixing time of 300 ms and an INEPT step as in Figure 3a were used. Experimental conditions were 600 MHz, 9 kHz MAS, 30 °C, and a t_1 proton evolution time of 2.9 ms. 1.5k scans were averaged for each time increment and processed as in Figure 3. Only inter-residue correlations are indicated.

proton line widths typically observed for rigid solids. These observations suggest that low frequency motions as previously detected for other membrane-associating peptides[70] here have a minor influence upon the dipolar (^{13}C,^{13}C) double-quantum excitation and that significant molecular motions are restricted to the cytoplasmic domain with correlation times in the range of 10^{-9} to 10^{-7}s.

Structural Analysis. The resonance assignments summarized in Table 1 (see Supporting Information) can be used to define conformation-dependent chemical shifts[71] under MAS conditions. Using only Cα and Cβ resonance assignments,[72] these values are used in Figure 8 to monitor protein secondary structure along the polypeptide sequence and are consistent with a trans-membrane α-helix proposed earlier.[30−32] For the cytoplasmic part, we find small secondary chemical shifts, suggesting that this domain does not exhibit a well-defined secondary structure. Notably, $\Delta\delta$ values for the ^{25}QARQ^{28} stretch close to the trans-membrane helix show β-strand character in qualitative agreement with early FTIR experiments.[35] Although this segment was detected in the dipolar correlation experiments, we do not find spectroscopic evidence for the formation of a β-sheet as discussed in ref 35. To construct a structural model of AFA-PLN in DMPC lipid bilayers, proton−proton distance constraints obtained from the HHC experiments were combined with dihedral angle constraints obtained from a TALOS-based analysis of the spectral assignments within CNS. The resulting conformation is depicted in Figure 9: a rather well-defined transmembrane α-helix, an extended hinge region, and a disordered N-terminal domain. Differences between the structural model depicted in Figure 9 and earlier NMR studies in organic solvents[30,31] and in detergent micelles,[32] which suggest the existence of a N-terminal α-helical domain, predominantly relate to the cytoplasmic segment of PLN. On the other hand, mutagenesis studies,[33] biophysical measurements,[28,34] and, in particular, EPR experiments[36] suggest that the cytoplasmic domain of AFA-PLN exists in a dynamic equilibrium of a

(69) Lee, M.; Goldburg, W. I. *Phys. Rev.* **1965**, *140*, 1261−1271.
(70) Davis, J. H.; Auger, M.; Hodges, R. S. *Biophys. J.* **1995**, *69*, 1917−1932.
(71) Wishart, D. S.; Sykes, B. D. *Methods Enzymol.* **1994**, *239*, 363−392.
(72) Luca, S.; Filippov, D. V.; van Boom, J. H.; Oschkinat, H.; de Groot, H. J. M.; Baldus, M. *J. Biomol. NMR* **2001**, *20*, 325−331.

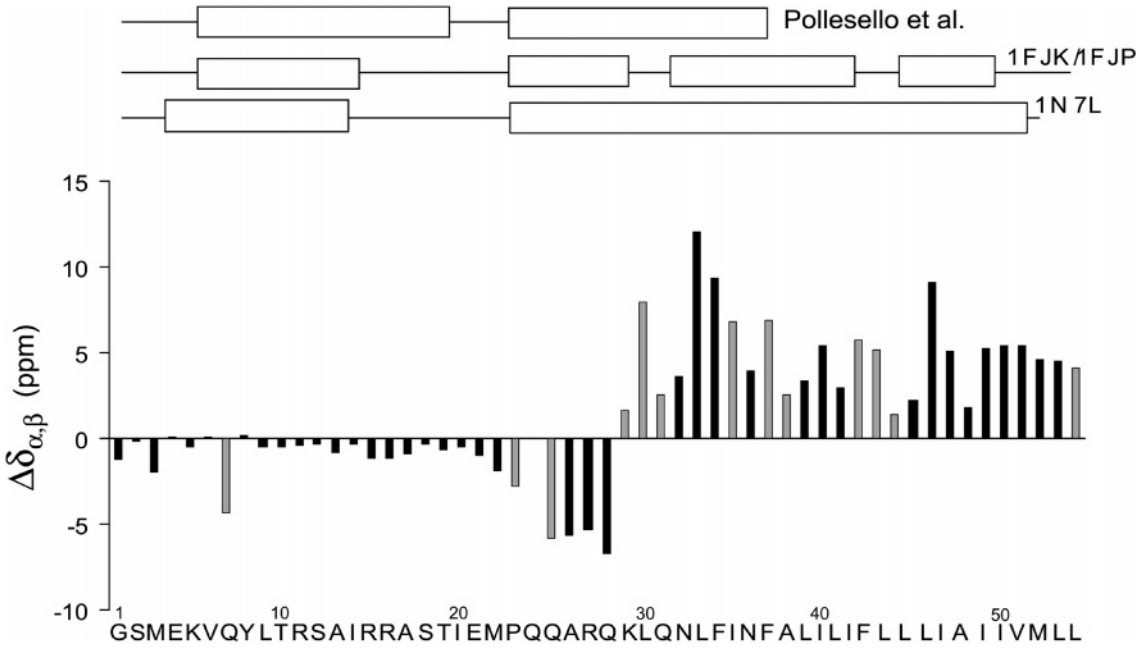

Figure 8. Comparison of solid-state NMR derived secondary chemical shifts $\Delta\delta$ (as defined in ref 72) to secondary structures resulting from solution-state NMR. For simplicity, only α-helical segments are indicated by rectangles. $\Delta\delta$ values are colored according to unequivocal spectral assignments (black) and tentatively assigned residues (gray). Additional details are given as Supporting Information.

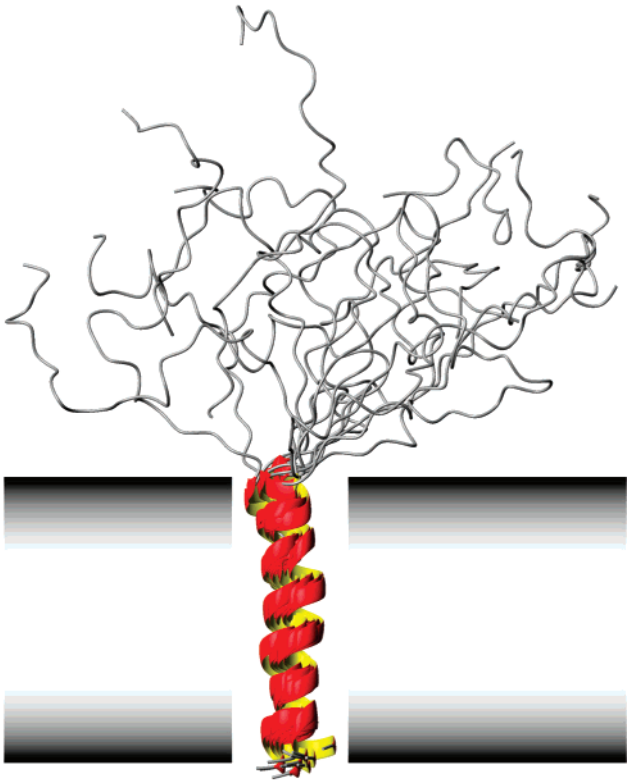

Figure 9. Structural model of AFA-PLN in DMPC lipid bilayers as seen by 2D MAS NMR. While the transmembrane α-helix is buried in the membrane, the cytoplasmic N-terminus exhibits a high degree of molecular disorder and is in close contact to an aqueous environment. An ensemble of 15 structures was selected to represent the molecular conformation of the PLN monomer. This figure was produced using MOLMOL.[73]

moderately stable α-helix and a significantly populated unstructured ensemble. Additional experiments conducted at low temperatures (data not shown) speak against the existence of such an additional α-helical N-terminal conformation of AFA-PLN in liposomes, but further studies, including the use of two-dimensional WISE[23] and exchange experiments, are planned to investigate different motional regimes at ambient temperatures.

4. Conclusions

In the present study, we have shown that complementary sets of NMR experiments can be devised to detect immobilized and flexible segments of a membrane protein studied under MAS conditions. While dipolar recoupling experiments are most effective for trans-membrane protein segments, molecular mobility was probed using T_2-selective through-bond correlation spectroscopy. These spectra were used to construct a structural model of the 52 amino acid protein phospholamban in lipid bilayers. While structural results obtained for the C-terminal segment of phospholamban corroborate earlier NMR studies in organic solvents and detergent micelles,[30−32] our MAS-based analysis is consistent with an N-terminal cytoplasmic domain that exhibits a high degree of structural disorder. While these findings are in agreement with other biophysical[36,74] and biochemical[25,33,75] results, the existence of a further population of membrane-associated phospholamban that contains an α-helical cytoplasmic domain as suggested by solution-state NMR[76] cannot be ruled out at present. Additional MAS-based correlation experiments that are sensitive to different motional regime are planned to elucidate these aspects in further detail. As recently demonstrated in polycrystalline molecules,[77] such experiments

(73) Koradi, R.; Billeter, M.; Wüthrich, K. *J. Mol. Graphics* **1996**, *14*, 51−60.
(74) Li, J. H.; Xiong, Y. J.; Bigelow, D. J.; Squier, T. C. *Biochemistry* **2004**, *43*, 455−463.
(75) Reddy, L. G.; Jones, L. R.; Cala, S. E.; Obrian, J. J.; Tatulian, S. A.; Stokes, D. L. *J. Biol. Chem.* **1995**, *270*, 9390−9397. Kimura, Y.; Kurzydlowski, K.; Tada, M.; MacLennan, D. H. *J. Biol. Chem.* **1996**, *271*, 21726−21731. Karim, C. B.; Marquardt, C. G.; Stamm, J. D.; Barany, G.; Thomas, D. D. *Biochemistry* **2000**, *39*, 10892−10897. Kimura, Y.; Asahi, M.; Kurzydlowski, K.; Tada, M.; MacLennan, D. H. *FEBS Lett.* **1998**, *425*, 509−512. Lockwood, N. A.; Tu, R. S.; Zhang, Z. W.; Tirrell, M. V.; Thomas, D. D.; Karim, C. B. *Biopolymers* **2003**, *69*, 283−292.
(76) Metcalfe, E. E.; Zamoon, J.; Thomas, D. D.; Veglia, G. *Biophys. J.* **2004**, *87*, 1205−1214.
(77) Seidel, K.; Etzkorn, M.; Sonnenberg, L.; Griesinger, C.; Sebald, A.; Baldus, M. *J. Phys. Chem. A* **2005**, *109*, 2436−2442.

could involve the detection of (scaled) one-bond dipolar ($^{13}C,^{1}H$) and (^{13}C, ^{13}C) interactions or the use of modified pulse schemes that permit a more quantitative determination of nuclear relaxation.

Monitoring through-space and through-bond polarization transfer in two complementary sets of NMR experiments as shown here not only provides access to the study of structure and dynamics under physiological conditions but also simplifies the spectroscopic analysis. Ongoing studies in our laboratory show that the pulse schemes discussed not only can be applied to proteoliposomes containing the 52-residue polypeptide phospholamban but can also be extended to study protein dynamics in larger membrane proteins or protein fibrils.

Acknowledgment. We thank Brigitta Angerstein and Petra Widawka for help with the sample preparation. Scientific discussions with Prof. C. Griesinger and Dr. C. E. Hughes are gratefully acknowledged. H.H. is a Liebig fellow of the Fonds der Chemischen Industrie. H.S.Y. is supported by the Heart and Stroke Foundation of Alberta, Canada.

Supporting Information Available: Spectral assignments of U-[$^{13}C,^{15}N$] AFA-PLN in DMPC bilayers, 2D slices of 3D HCC data sets, 2D INEPT data for (i) two different lipid compositions, (ii) two different lipid-to-protein ratios, and (iii) for AFA-PLN−DOPC/DOPE liposomes before and after lyophilization and rehydration, and ^{31}P MAS NMR data of AFA-PLN/DMPC proteoliposomes. This material is available free of charge via the Internet at http://pubs.acs.org.

JA0530164